ACS APPLIED MATERIALS & INTERFACES

www.acsami.org

Research Article

# Stability of N-Heterocyclic Carbene Monolayers under Continuous Voltammetric Interrogation

Miguel Aller Pellitero,[‖] Isabel M. Jensen,[‖] Nathaniel L. Dominique,[‖] Lilian Chinenye Ekowo, Jon P. Camden,* David M. Jenkins,* and Netzahualcóyotl Arroyo-Currás*

Cite This: *ACS Appl. Mater. Interfaces* 2023, 15, 35701−35709

Read Online

ACCESS | Metrics & More | Article Recommendations | Supporting Information

**ABSTRACT:** N-Heterocyclic carbenes (NHCs) are promising monolayer-forming ligands that can overcome limitations of thiol-based monolayers in terms of stability, surface functionality, and reactivity across a variety of transition-metal surfaces. Recent publications have reported the ability of NHCs to support biomolecular receptors on gold substrates for sensing applications and improved tolerance to prolonged biofluid exposure relative to thiols. However, important questions remain regarding the stability of these monolayers when subjected to voltage perturbations, which is needed for applications with electrochemical platforms. Here, we investigate the ability of two NHCs, 1,3-diisopropylbenzimidazole and 5-(ethoxycarbonyl)-1,3-diisopropylbenzimidazole, to form monolayers via self-assembly from methanolic solutions of their trifluoromethanesulfonate salts. We compare the electrochemical behavior of the resulting monolayers relative to that of benchmark mercaptohexanol monolayers in phosphate-buffered saline. Within the −0.15 to 0.25 V vs AglAgCl voltage window, NHC monolayers are stable on gold surfaces, wherein they electrochemically perform like thiol-based monolayers and undergo similar reorganization kinetics, displaying long-term stability under incubation in buffered media and under continuous voltammetric interrogation. At negative voltages, NHC monolayers cathodically desorb from the electrode surface at lower bias (−0.1 V) than thiol-based monolayers (−0.5 V). At voltages more positive than 0.25 V, NHC monolayers anodically desorb from electrode surfaces at similar voltages to thiol-based monolayers. These results highlight new limitations to NHC monolayer stability imposed by electrochemical interrogation of the underlying gold electrodes. Our results serve as a framework for future optimization of NHC monolayers on gold for electrochemical applications, as well as structure−functionality studies of NHCs on gold.

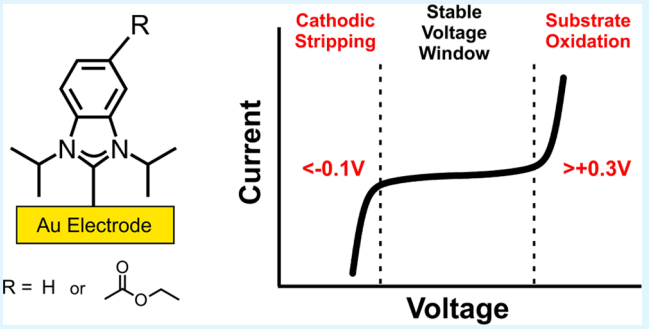


**KEYWORDS:** *N-heterocyclic carbenes, monolayer self-assembly, monolayer stability, thiols, voltammetry, electrochemical sensors, monolayer reorganization, carbene salts*

## INTRODUCTION

Monolayer-forming chemistries are critical components of biosensing interfaces.[1−3] They offer the functionality to conjugate biomolecular receptors to detection interfaces,[4,5] prevent nonspecific protein adsorption,[6−8] and, in the case of electrochemical platforms, dampen undesired currents from background electrochemical processes.[9−11] To date, the most commonly used monolayers for biosensor interfaces are based upon thiol-on-gold self-assembly.[12−14] The resulting thiol monolayers have been heavily researched, are well understood, and are an affordable and convenient option for rapid prototyping of biosensing platforms. Unfortunately, thiol-based monolayers are labile and can quickly decay in biological systems via various mechanisms including voltage-induced desorption,[15,16] competitive displacement (by naturally occurring thiols like cysteine),[17] and biofouling.[18] All of these mechanisms can occur simultaneously, severely limiting the operational life of thiol-based monolayers to hours or, in best cases, a few days.[19] For electrochemical systems specifically, the rate of decay is dramatically accelerated by the continuous application of voltage perturbations,[15,17] which can affect not only the monolayer chemistries themselves but also the underlying gold substrates. Thus, there is interest in developing novel monolayer-forming chemistries that overcome the limitations of thiols to enable continuous biosensor operation over periods of weeks or months or under extreme chemical environments.

Chemistries based on N-heterocyclic carbenes (NHCs) are emerging as promising alternatives to thiols for monolayer

Received: April 28, 2023
Accepted: June 28, 2023
Published: July 14, 2023

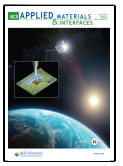





https://doi.org/10.1021/acsami.3c06148
*ACS Appl. Mater. Interfaces* 2023, 15, 35701−35709

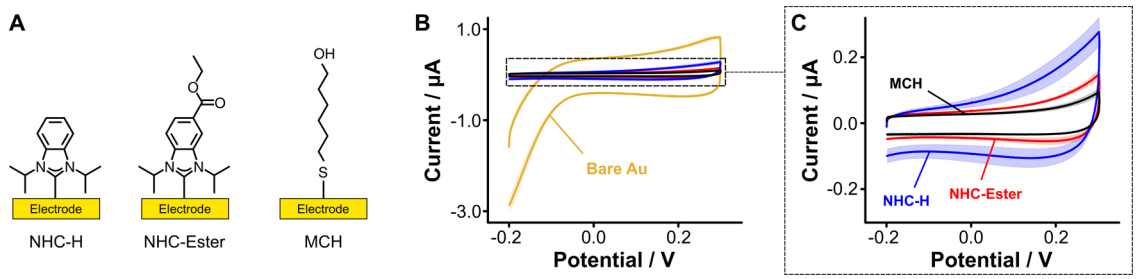


**Figure 1.** Monolayer-forming chemistries used in this study. (A) 1,3-Diisopropylbenzimidazole (NHC-H), 5-(ethoxycarbonyl)-1,3-diisopropylbenzimidazole (NHC-ester), and mercaptohexanol (MCH). (B) Decrease in voltammetric charging and oxygen reduction currents caused by monolayer formation. The yellow line illustrates the typical charging current of a bare gold electrode in the absence of any monolayer coatings and the faradic current from dissolved oxygen reduction starting at −0.1 V. (C) Zoomed-in region showing differences in voltammetric charging currents between the three monolayers considered in this work following overnight deposition at 25 °C from methanolic solutions of the NHC triflate salts and alkylthiol. Solid lines represent the average of 4 electrodes. Shaded areas represent their standard deviation. All voltammograms measured at a scan rate of 100 mV $s^{-1}$. Voltages in all figures are reported vs Ag|AgCl.

formation.[20,21] Their strong sigma donor strength and affinity for gold and other transition-metal surfaces have made NHCs valuable monolayer-forming candidates for applications in surface chemistry that require long-term stability and added reactivity for efficient bioconjugations. For example, NHCs have been used to support biosensors,[22−25] improve heterogeneous catalysis,[26−30] and passivate reactive surfaces.[31−37] Indeed, their robust stability under biological conditions[38] also makes them excellent candidates for biosensing applications[23,39] and, in particular, for electrochemical sensing strategies intended for deployment in biofluids.

A variety of methods have been utilized for the deposition of Au-NHC monolayers. The first monolayers were formed via deprotonation using a strong base under air-free conditions (i.e., the "free-carbene" method)[20,21] or via vacuum deposition (e.g., from $CO_2$ or bicarbonate adducts).[22,40] More recent reports utilize electrochemical deposition[41] or incubation in a methanolic solution containing the bicarbonate[22] or triflate/mesylate[24,25,42] salts of the NHC. These milder conditions allow for the deposition of NHCs possessing the protic functional groups (i.e., amines and carboxylates) necessary for coupling reactions. However, despite their great promise, much remains unknown regarding NHC monolayer organization and stability under voltage perturbations such as those performed in voltammetry. Specifically, stability limits in terms of maximum voltage tolerance and monolayer desorption kinetics have not been explored to date, leaving an important gap in knowledge that limits technology adoption in advanced electrochemical sensing platforms such as continuous molecular monitors.

Seeking to expand the understanding of NHC monolayer formation, stability, and performance in electrochemical systems, this study addresses three primary objectives: first, the evaluation of gold electrode surface coverage by NHC monolayers formed via spontaneous assembly from methanolic solutions of their trifluoromethanesulfonate (triflate) salts compared to benchmark monolayers of mercaptohexanol (MCH); second, determination of the most suitable voltage window for electrochemical sensors based on NHC monolayers before either cathodic or anodic desorption occurs; and third, assessment of the stability of the resulting NHC monolayers in phosphate-buffered saline in the absence of voltage perturbations, as well as the effect of serial voltammetric interrogation on monolayer organization. To pursue these objectives, we synthesized two model NHC compounds (Figure 1A): 1,3-diisopropylbenzimidazole (NHC-H) and 5-(ethoxycarbonyl)-1,3-diisopropylbenzimidazole (NHC-ester). The NHC-H moiety is one of the most thoroughly studied N-heterocyclic carbenes for self-assembly of monolayers (SAMs) on gold and is often considered the reference NHC for gold surface studies;[21] thus, it represents an excellent baseline for NHCs under electrochemical interrogation. Additionally, previous electrochemical studies by Crudden et al. employed the NHC-ester, which was attached to electrodes via the triflate deposition method.[24] Changes in sterics and electronics due to the ester functionalization of the NHC backbone provide a comparison of electrochemical stability between the two related NHCs. Finally, the NHC-ester works as a simple model ligand toward the kinds of NHCs that could be post-synthetically modified for amide-coupling reactions.[21,24]

## RESULTS AND DISCUSSION

**N-Heterocyclic Carbenes Spontaneously Adsorb on the Surface of Gold Electrodes.** A joint approach of electrochemical and spectroscopic methods was used to evaluate the spontaneous formation of NHC monolayers. Electrochemical evaluation of the NHC monolayer was determined by probing three key features: the capacitive current, the faradic contribution of oxygen reduction, and the faradic contribution of gold oxidation.

We assessed the capacitive currents of gold electrodes with and without NHC monolayers via cyclic voltammetry. The electrode−monolayer−electrolyte interface can be represented as a parallel plate capacitor,[43,44] where the electrode and the electrolyte correspond to the capacitor plates and the monolayer to the dielectric in between. In the absence of a monolayer, the dielectric consists of water molecules and solvated ions at the electrode−electrolyte interface, and the capacitance is large due to the diffuse layer of ions aligning to any applied electric fields. However, in the presence of a monolayer, the spacing between the electrode and the electrolyte increases, dropping capacitive currents. Following this model, the monolayer thickness and dielectric constant determine the magnitude of capacitive currents at the electrode. Therefore, any organizational changes due to the formation, redistribution, or loss of monolayer elements can strongly affect dielectric length (changes in the number and


https://doi.org/10.1021/acsami.3c06148
ACS Appl. Mater. Interfaces 2023, 15, 35701−35709

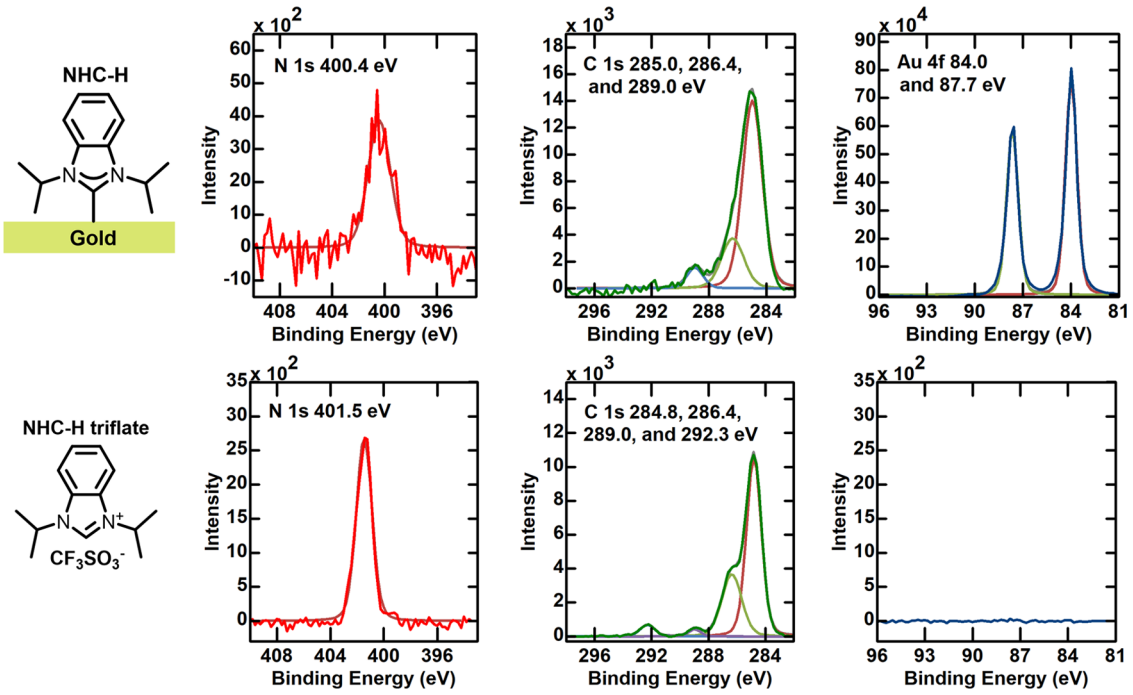


**Figure 2.** X-ray photoelectron spectroscopy confirms that NHC monolayers are formed by chemisorption on gold electrodes. Top: spectra of electrode-bound NHC-H showing the diagnostic N 1s transition with BE = 400.4 eV. The N 1s transition is in agreement with previous studies indicating a chemisorbed carbene between 399.9 and 401 eV.[42,47,48] Bottom: spectra of NHC-H triflate salt showing N 1s transition with binding energy BE = 401.5 eV. The N 1s transition is in agreement with previous studies of unbound NHC salts at >401 eV.[49,50]

spatial orientation of elements) and dielectric constant, changing capacitive currents.[10,16,17,45]

As a second, parallel assessment of monolayer formation, we monitored the faradic contribution from oxygen reduction to the total voltammetric currents measured at voltage biases more negative than −0.1 V (vs AglAgCl). Dissolved molecular oxygen undergoes a gold-catalyzed bond breaking via inner-sphere electron transfer (yellow trace in Figure 1B),[46] increasing the faradic current when monolayers are porous or when monolayer elements are cleaved or desorbed from the electrode surface during voltammetric interrogation.[10,16,17] And third, we evaluated the faradic contribution from gold oxidation[3] to the currents measured at voltage biases more positive than 0.25 V, wherein the gold electrode surface itself becomes oxidized. This three-pronged strategy allowed us to get a clear electrochemical picture of the quality of NHC monolayers on polycrystalline gold electrodes and their stability under continuous voltammetric interrogation.

Using the above-described strategy, we demonstrate that NHCs form monolayers on polycrystalline gold surfaces that achieve an extent of surface passivation that is comparable to that attained by benchmark MCH monolayers. To show this effect, we prepared monolayers on gold disk electrodes via 4 h long incubation under vigorous stirring in methanolic solutions of NHC-H, NHC-ester, and MCH (Figure 1A). After rinsing with water, we immersed the freshly functionalized electrodes into phosphate-buffered saline and interrogated them via cyclic voltammetry at a voltage scanning rate of 100 mV $s^{-1}$. The resulting voltammograms showed a multifold decrease in capacitive currents relative to measurements on unfunctionalized gold electrodes and a complete suppression of oxygen reduction currents at voltages below −0.1 V (Figure 1B). A closer inspection of monolayer voltammograms revealed that NHC-ester monolayers achieved surface passivation that is comparable to that of MCH monolayers (Figure 1C), as indicated by the capacitive currents of the two systems measured at +0.15 V ($i_{C,NHC\text{-}ester}$ = 110 ± 10 nA vs $i_{C,MCH}$ = 72 ± 7 nA). In contrast, NHC-H monolayers presented larger capacitive currents ($i_{C,NHC\text{-}H}$ = 190 ± 60 nA). These results can be explained by the longer tail of the NHC-ester, which may contribute to increasing dielectric length, thereby decreasing capacitive currents relative to the unmodified NHC-H. The results also indicate that NHCs spontaneously form adsorbed layers on gold electrodes with packing densities able to suppress the electrochemical reduction of dissolved oxygen, as no cathodic currents are observed at voltages below 0.0 V (Figure 1B,C).

To confirm that the monolayers formed by spontaneous assembly from methanolic solutions of NHC triflate salts are chemisorbed on the surface of gold electrodes, we measured the presence of NHC-related nitrogens on the electrode surface ex situ, after monolayer assembly via X-ray photoelectron spectroscopy (XPS). The resulting XPS spectra of the NHC monolayer-coated electrode surface showed an N 1s transition with binding energy BE = 400.4 eV (Figure 2, top), in excellent agreement with previous studies, indicating that chemisorbed carbenes display N 1s transitions between 399.9 and 401 eV.[42,47,48] This shift is to lower energy from the N 1s transition seen in solid NHC-H triflate salt, with BE = 401.5 eV (Figure 2, bottom), in agreement with previous studies of unbound NHC salts.[49,50] Quantitative analysis of the XPS data illustrates that the N 1s to Au 4f peak ratios are comparable with previous triflate/mesylate deposition protocols (Figure S1 and Table S1).[24,25,42] These results confirm the presence of chemisorbed NHC monolayers of comparable quality to previous reports on the surface of our gold electrodes.

**Assessment of the Voltage Window for NHC Monolayers.** The stability of self-assembled monolayers


https://doi.org/10.1021/acsami.3c06148
ACS Appl. Mater. Interfaces 2023, 15, 35701−35709

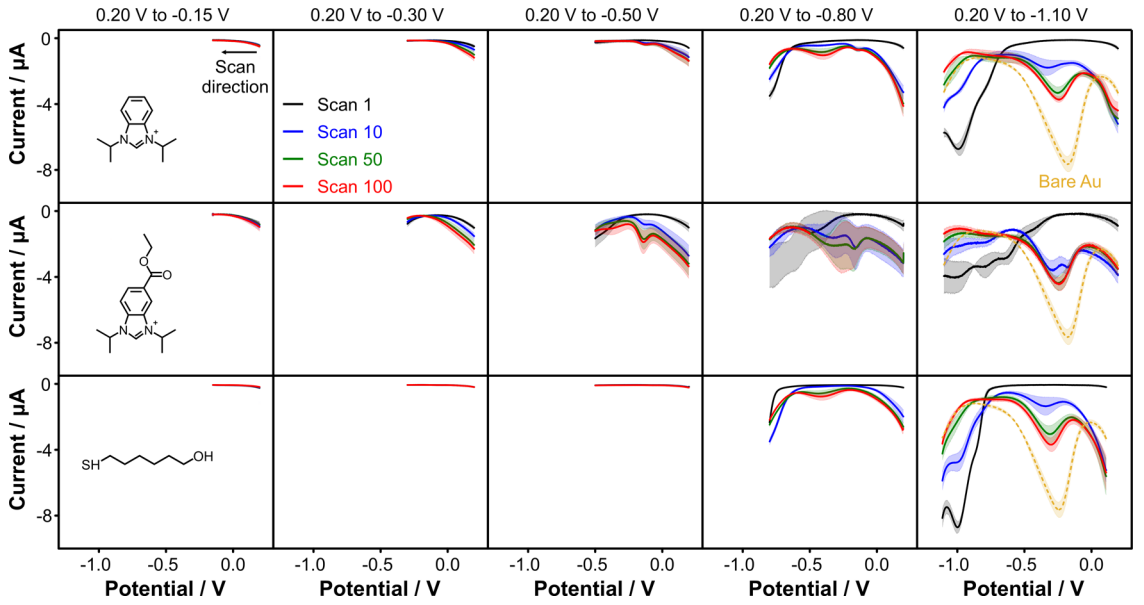


**Figure 3.** Desorption of NHC monolayers under negative voltage bias. Monolayer stability on the surface of polycrystalline gold electrodes is a function of voltage bias. For (A) NHC-H and (B) NHC-ester monolayers, cathodic desorption starts to occur at voltages more negative than −0.15 V in phosphate-buffered saline. This is seen as a progressive increase in background current (at 0.20 V) and the eventual appearance of oxygen reduction peaks (at −0.20 V). For reference, oxygen reduction on bare gold electrodes is shown in yellow at the rightmost panels. (C) In contrast, benchmark MCH monolayers are more tolerant to negative voltage biasing, not showing signs of increased background currents or oxygen reduction until voltage biases more negative than −0.50 V are applied. Square wave voltammograms measured at a frequency of 50 Hz, amplitude of 50 mV, and a step size of 1 mV. Solid lines represent the average of 4 electrodes. Shaded areas represent their standard deviation.

strongly depends on the voltage applied to the electrode,[51] which defines their most suitable voltage window for electrochemical sensing. To study the stability of NHC monolayers at different voltage biases and assess a functional voltage window, we first investigated the cathodic desorption of NHC monolayers by systematically sweeping the voltage to increasingly more negative values via square wave voltammetry (SWV). By using SWV, we differentially remove the charging current from the voltammograms, thus achieving more sensitive measurements of faradic processes, in this case, the reduction of dissolved molecular oxygen.[10] For these experiments, we prepared five batches of four electrodes per monolayer and interrogated them starting at a voltage of 0.20 V and then sweeping negatively to −0.15 V for batch 1, −0.30 V for batch 2, −0.50 V for batch 3, −0.80 V for batch 4, and −1.10 V for batch 5. To monitor stability, we performed 100 scans across each voltage window (Figure 3).

Our results show that voltage sweeping below −0.15 V causes rapid desorption of NHC monolayers, with the NHC-ester desorbing faster than the NHC-H. This desorption is seen as an increase in capacitive currents plus the appearance of oxygen reduction waves at ∼−0.2 V when the voltage is negatively biased to −0.5 V (see the third column in Figure 3). For reference, we show the position of the oxygen reduction wave on bare gold electrodes in the last column (yellow trace), which appears at −0.2 V. In addition, at voltages more negative than −0.5 V, we observed the appearance of stripping waves in the first scan (black traces), which caused rapid monolayer desorption as visible in subsequent scans. MCH monolayers, in contrast, easily tolerated voltage biasing as negative as −0.5 V, without signs of monolayer desorption within 100 voltammetric scans (bottom of the third column in Figure 3C). Instead, they started to desorb at more negative voltages but also showed stripping peaks at −1.0 V like NHC monolayers. These results indicate that MCH monolayers are more resistant to cathodic stripping than the NHC monolayers studied in this work.

We next investigated the stability of NHC monolayers when subjected to positive voltage biases (Figure 4). These experiments were performed under identical conditions to those employed in Figure 3. In more detail, we prepared three batches of four electrodes per monolayer and interrogated them starting at a voltage of −0.15 V, thus preventing monolayer removal and then sweeping positively to 0.3 V for batch 1, 0.5 V for batch 2, and 0.7 V for batch 3. The resulting voltammograms indicate that, regardless of the ligand used, all monolayers desorb when the applied voltage is more positive than 0.3 V (Figure 4). This is a limit imposed by the underlying gold electrode, which undergoes fractional surface oxidation (presumably to singly oxygenated species such as Au−OH or Au−O)[3] at an onset potential of 0.3 V.

**N-Heterocyclic Carbenes Can Form Monolayers That Are Stable for Days.** To investigate the stability of the NHC monolayer, we immersed NHC-functionalized electrodes in phosphate-buffered saline and performed discreet voltammetric interrogations once every day for 7 days. To favor any passive desorption of the monolayers, we immersed the modified electrodes in microcentrifuge tubes containing the same buffer and stirred them vigorously at 700 rpm and 25 °C using a ThermoMixer. Based on the voltage limits obtained from Figures 3 and 4, we performed electrochemical measurements using a voltage window between −0.05 and 0.30 V, thus preventing any voltage-induced desorption of the monolayers. When inspecting the resulting voltammograms at $t$ = 0 h and $t$ = 168 h (7 days), we observed no statistically significant changes in capacitive currents across NHC-H (Figure 5A), NHC-ester (Figure 5B), or MCH monolayers (Figure 5C). Another way to visualize this information is by


https://doi.org/10.1021/acsami.3c06148
ACS Appl. Mater. Interfaces 2023, 15, 35701−35709

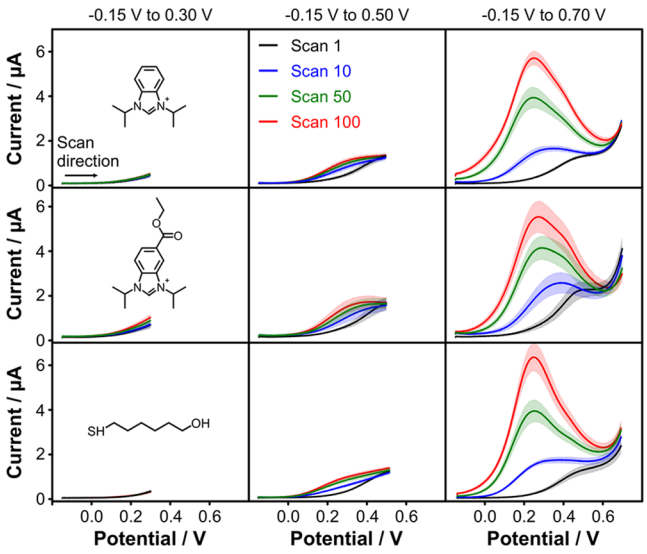


**Figure 4.** Desorption of NHC monolayers under positive voltage bias. For (A) NHC-H and (B) NHC-ester monolayers, anodic desorption starts to occur at voltages more positive than 0.2 V in phosphate-buffered saline. This is seen as a progressive increase in currents from surface gold oxidation (at 0.25 V). (C) Under positive voltage bias, benchmark MCH monolayers also undergo anodic desorption under similar conditions. Square wave voltammograms measured at a frequency of 50 Hz, amplitude of 50 mV, and a step size of 1 mV. Solid lines represent the average of 4 electrodes. Shaded areas represent their standard deviation.

extracting the magnitude of the capacitive currents at a probe voltage of 0.15 V once a day and use them to build sensorgrams as illustrated in Figure 5D−F. These sensorgrams highlight that all three monolayers do not change over the 7 day period considered. Performing linear regression analyses of the sensorgrams shows poor correlation to a line (average $R^2 \sim 0.4$), as expected for random data dispersion originating from background noise in the capacitive measurements. In other words, the changes in current over time are negligible. Additionally, they show that packing is comparably good across all three chemistries, with the NHC monolayers presenting higher charging currents on average but within a factor of two from MCH monolayers.

Another critical aspect of electrochemical sensors is their stability under continuous voltammetric interrogation. The voltage bias applied during continuous interrogation can influence the stability of the Au−C and Au−S bonds, leading to progressive monolayer removal.[17] To study this, we prepared new batches of NHC- and MCH-coated electrodes and serially interrogated them by cyclic voltammetry every 10 s for 7 days (60,500 cycles in total). For this test, we used a voltage window from −0.05 to +0.25 V to avoid the voltage-induced desorption processes seen in Figures 3 and 4. Voltammograms recorded before and after 168 h of continuous interrogation show that, across this voltage window, NHC and MCH monolayers are stable as no increases in capacitive currents are observed (Figure 6A−C). Interestingly, under these conditions, NHC monolayers seem to undergo a significant voltage-induced reorganization, as showed by the decrease in capacitive current at 0.15 V in the sensorgrams observed for both NHCs (Figure 6D,E), leading to values comparable to those obtained for MCH monolayers ($i_{C,MCH} \sim$ 55 nA, Figure 6F). We speculate that this significant decrease in capacitive currents reflects a field-induced monolayer reorganization, where some NHC molecules may change orientation on the electrode surface, thereby changing dielectric length. This effect is more noticeable for the NHC-H monolayer (from $i_{C,NHC-H} \sim$ 140 nA to $i_{C,NHC-H} \sim$

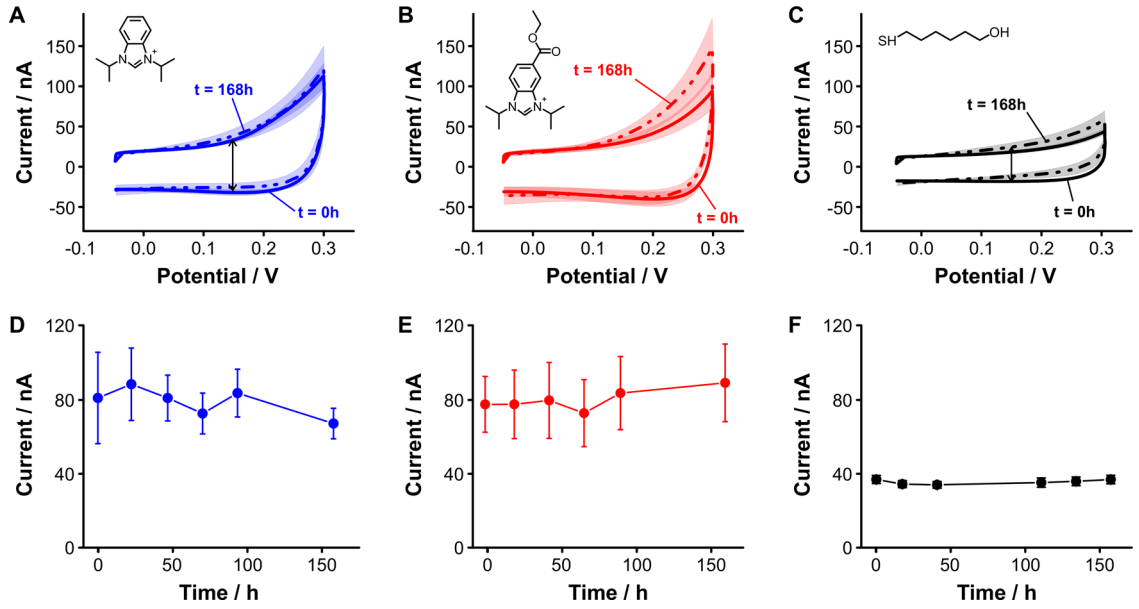


**Figure 5.** Monolayer reorganization in undisturbed buffered solutions as seen via discreet voltammetric interrogation. Top panels show cyclic voltammograms of (A) MCH, (B) NHC-ester, and (C) NHC-H monolayers on polycrystalline gold electrodes measured at $t$ = 0 h and $t$ = 168 h (7 days) of incubation in phosphate-buffered saline at 25 °C. Bottom panels show voltammetric charging currents sampled at 0.15 V once a day, except for the last measurement, which was recorded after 3 days to skip the weekend for (D) NHC-H, (E) NHC-ester, and (F) MCH monolayers. Solid lines represent the average of 4 electrodes. Shaded areas represent their standard deviation. Dotted lines represent a linear regression of the data with correlation coefficients $R^2$ = 0.518, $R^2$ = 0.576, and $R^2$ = 0.111 for NHC-H, NHC-ester, and MCH, respectively. All voltammograms were measured at a scan rate of 100 mV $s^{-1}$.


https://doi.org/10.1021/acsami.3c06148
ACS Appl. Mater. Interfaces 2023, 15, 35701−35709

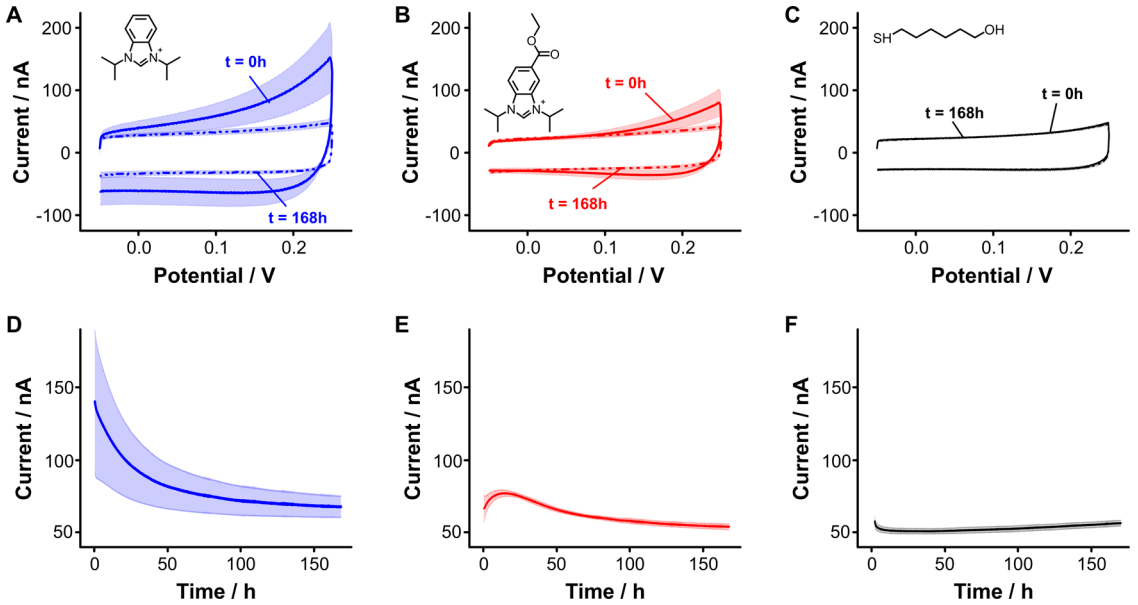


**Figure 6.** Monolayer reorganization under continuous voltammetric interrogation. Top panels show cyclic voltammograms of (A) NHC-H, (B) NHC-ester, and (C) MCH monolayers on polycrystalline gold electrodes measured at $t$ = 0 h and $t$ = 168 h (7 days) of incubation in phosphate-buffered saline at 25 °C. Bottom panels show voltammetric charging currents sampled at 0.15 V every 10 s for (D) NHC-H, (E) NHC-ester, and (F) MCH monolayers. Solid lines represent the average of 4 electrodes. Shaded areas represent their standard deviation. All voltammograms measured at a rate of 100 mV $s^{-1}$.

70 nA) than the NHC-ester monolayer (from $i_{C,NHC\text{-}ester} \sim 60$ nA to $i_{C,NHC\text{-}ester} \sim 55$ nA). Investigation of gold surfaces with and without NHC-based monolayers via scanning electron microscopy (SEM, Figure S2) and energy-dispersion spectroscopy (EDS, Figure S3) revealed no changes in surface morphology or composition due to voltammetric scanning, a strong indication that the capacitive changes observed are due to monolayer reorganization. However, future spectroscopic measurements beyond the scope of this work are needed to further clarify such effects.

## CONCLUSIONS

We evaluated the ability of NHCs to form self-assembled monolayers from their triflate salts under open-circuit conditions and investigated the quality of such monolayers relative to benchmark MCH monolayers via electrochemistry. Additionally, we investigated the useful voltage window of such monolayers to identify limits where anodic or cathodic desorption can occur. Our results indicate that NHCs form monolayers that passivate the surface of gold electrodes to a similar extent compared to benchmark mercaptohexanol chemistry. However, the voltage window available for electrochemical interrogation is shorter in NHC relative to MCH-based monolayers. Specifically, NHC-based monolayers display an operational voltage window of roughly 450 mV, from −0.15 to 0.3 V vs Ag|AgCl. Although this voltage window is considerably shorter than that of MCH monolayers (from −0.5 to 0.3 V vs Ag|AgC), stable electrochemical measurements for sensing applications can potentially be achieved by selecting a redox reporter with a formal redox potential close to 0 V. For example, redox mediators like *N*,*N*,*N*′,*N*′-tetramethyl-*p*-phenylenediamine (TMPD),[52] tetrathiafulvalene (TTF),[53] and Os(II/III)[54] have redox potentials that fall in a suitable voltage window for use with NHC-based monolayers. Future investigations are needed to clarify if the choice of the electrochemical technique and technique parameters can also affect NHC monolayer stability and to what extent.

## METHODS

**Chemicals.** 5-Benzimidazole carboxylic acid, 2-bromopropane, 2-iodopropane, sodium carbonate, sodium sulfate, sulfuric acid, ethyl acetate, acetonitrile, isopropanol, methylene chloride, and phosphate-buffered saline (PBS) (11.9 mM $HPO_3^{2-}$, 137 mM NaCl, 2.7 mM KCl; pH = 7.4) were purchased from Fisher Scientific (Waltham, MA). Sodium hydroxide, methanol, pyridine, benzimidazole, and 6-mercapto-1-hexanol were purchased from Sigma-Aldrich (St. Louis, MO). Trifluoromethanesulfonate anhydride was acquired from Oakwood Chemical (Estill, SC). Cesium carbonate was acquired from Thermo Fisher Scientific (Waltham, MA), and ethanol 200 proof was purchased from Decon Labs (King of Prussia, PA). Platinum counterelectrodes (cat. #012961) and gold disk electrodes (cat. #002314, Ø = 1.6 mm) were purchased from ALS (Tokyo, Japan). Ag|AgCl (1 M KCl) reference electrodes were purchased from CH Instruments (Austin, TX). 1200/P2500 silicon carbide grinding paper (36-08-1200) was purchased from Buehler (Lake Bluff, IL), and cloth pads with alumina slurry (CF-1050) were purchased from BASi (West Lafayetter, IN). A ThermoMixer C was purchased from Eppendorf (Framingham, MA). Gold and Chromium pellets were purchased from Kurt J. Lesker (Jefferson Hills, PA). Carbon tape (cat. #77819-65) for XPS analysis was purchased from Electron Microscopy Sciences (Hatfield, PA).

**NHC Synthesis.** Synthesis of the NHC-H started from benzimidazole.[55] The $^1$H, $^{13}$C, and $^{19}$F NMR for the synthesized compound matched previously reported values (Figures S4−S6).[56,57] We also include mass spectra to confirm structural identity via molecular ion identification (Figure S7). Synthesis of NHC-ester was performed starting from the 5-benzimidazole carboxylic acid following a previously published method.[55] The $^1$H, $^{13}$C, and $^{19}$F NMR for the synthesized compound (Figures S8−S10) matched previously reported values.[55] We also include mass spectra to confirm structural identity via molecular ion identification (Figure S11).

**Electrode Preparation.** We polished the gold electrodes using silicon carbide paper and a cloth pad with alumina slurry for ∼2 min. After polishing, we rinsed the electrodes with deionized water and sonicated them in water for 30 s to remove debris. Next, we cleaned


https://doi.org/10.1021/acsami.3c06148
ACS Appl. Mater. Interfaces 2023, 15, 35701−35709

their surfaces by cyclic voltammetry first in 0.5 M NaOH, scanning from −0.3 to −1.6 V, and then in 0.5 M $H_2SO_4$, scanning from 0 to +1.6 V, a total of 200 scans at 0.5 V $s^{-1}$ in each solution.[16] We then rinsed the electrodes once with deionized water and once with methanol and placed them into 10 mM methanolic solutions of either the NHCs or MCH ligands under vigorous stirring (1500 rpm) at 25 °C. Monolayer deposition times were investigated via monitoring of voltammetric charging currents after deposition times of 2, 4, and 15 h (Figure S12). Based on these data, we selected a deposition time of 4 h because charging currents were within one standard deviation of each other between 4 h and 15 h long depositions. Following the electrode modification, we rinsed the electrodes with deionized water.

**Electrochemical Measurements.** A CH Instruments Electrochemical Analyzer (CHI 1040C, Austin, TX) multichannel potentiostat and associated software were used for all electrochemical measurements. A three-electrode cell configuration consisting of a gold working electrode, coiled platinum wire counterelectrode, and AglAgCl reference electrode was used. In this work, continuous voltammetric interrogation refers to the serial interrogation of sensors via either cyclic or square wave voltammetry, using a wait period of 10 s between voltage sweeps. Voltammograms were processed via SACMES, an open-access software previously reported by our group[58] that allows batch extraction of capacitive currents from voltammogram datasets.

**XPS Measurements.** XPS measurements were obtained with a PHI VersaProbe II surface analysis instrument from Physical Electronics (Chanhassen, MN) equipped with a monochromatic Al K$\alpha$ X-ray source (photon energy = 1486.6 eV). High-resolution spectra were obtained for at least two sample spots using a 23.50 eV pass energy under ultrahigh vacuum conditions. For the N 1s, C 1s, and Au 4f high-resolution spectra of NHC triflate salts, we performed 20, 10, and 7 sweeps, respectively. For the N 1s, C 1s, and Au 4f high-resolution spectra of NHC-treated gold films, we performed 30, 20, and 20 sweeps, respectively. Spectra acquired on gold film surfaces were summed together and calibrated vs the binding energy of the Au 4f peak at 83.98 eV,[59] whereas spectra acquired on carbon tape were calibrated versus the binding energy of the C 1s peak at 284.8 eV.[60] The spectra for N 1s, C 1s, and Au 4f were then background-subtracted using a linear,[61] Shirley,[62] or Tougard background subtraction,[63] and peak locations were determined with a Voigt Model in CasaXPS.[62] XPS data were analyzed using the Handbook of X-ray Photoelectron Spectroscopy.[59]

For XPS data of gold electrode surfaces, a gold film substrate was used for all experiments. Briefly, 5 nm of chromium was deposited onto a glass microscope slide, followed by 100 nm of gold using a physical vapor deposition system (Nano36, Kurt J. Lesker). Prior to deposition, microscope slides were etched using piranha acid (caution, extremely dangerous) made with a 4:1 ratio of conc. sulfuric acid to 30% hydrogen peroxide and rinsed with copious amounts of water. Gold films were electrochemically activated (vide supra) and rinsed with water and HPLC-grade methanol before use. Minor delamination at the edges of the gold film was observed after the electrochemical activation in sulfuric acid, but the majority of the film remained affixed to the substrate. The gold film was soaked in the triflate solution overnight and rinsed with ultrapure water (>18 MΩ) prior to analysis. The gold film was mounted for XPS analysis using a strip of copper to ground and immobilize the sample. For XPS data of the NHC triflate salt, the powder was gently pressed into a piece of carbon tape using a plastic spatula. Then, samples were mounted by affixing the carbon tape onto the sample stage. XPS survey scans are shown in Figures S13 and S14.

**Scanning Electron Microscopy (SEM) and Energy-Dispersive Spectroscopy (EDS) Analysis.** Gold (111) substrates (Ultra-Flat Gold Surfaces, Platypus Technologies, Fitchburg, WI) were utilized for SEM and EDS experiments. SEM images were collected using a FEI Magellan 400 field emission SEM in immersion mode with a circular backscattering detector. EDS spectra were collected using 5 keV accelerating voltage in the SEM instrument and a Bruker XFlash 5010 X-ray detector. Peak assignment was performed using X-ray data presented by Bearden.[64]

## ■ ASSOCIATED CONTENT

### Supporting Information

The Supporting Information is available free of charge at https://pubs.acs.org/doi/10.1021/acsami.3c06148.

Materials and measurements (Figures S1−S14) and XPS data (Table S1) (PDF)

## ■ AUTHOR INFORMATION


### Corresponding Authors

**Jon P. Camden** − *Department of Chemistry and Biochemistry, University of Notre Dame, Notre Dame, Indiana 46556, United States;* orcid.org/0000-0002-6179-2692; Email: jon.camden@nd.edu

**David M. Jenkins** − *Department of Chemistry, University of Tennessee, Knoxville, Tennessee 37996, United States;* orcid.org/0000-0003-2683-9157; Email: jenkins@ion.chem.utk.edu

**Netzahualcóyotl Arroyo-Currás** − *Department of Pharmacology and Molecular Sciences, Johns Hopkins University School of Medicine, Baltimore, Maryland 21205, United States;* orcid.org/0000-0002-2740-6276; Email: netzarroyo@jhmi.edu

### Authors

**Miguel Aller Pellitero** − *Department of Pharmacology and Molecular Sciences, Johns Hopkins University School of Medicine, Baltimore, Maryland 21205, United States;* orcid.org/0000-0001-8739-2542

**Isabel M. Jensen** − *Department of Chemistry, University of Tennessee, Knoxville, Tennessee 37996, United States*

**Nathaniel L. Dominique** − *Department of Chemistry and Biochemistry, University of Notre Dame, Notre Dame, Indiana 46556, United States;* orcid.org/0000-0002-0439-9982

**Lilian Chinenye Ekowo** − *Department of Chemistry and Biochemistry, University of Notre Dame, Notre Dame, Indiana 46556, United States;* orcid.org/0000-0002-1731-0879

Complete contact information is available at: https://pubs.acs.org/10.1021/acsami.3c06148


### Author Contributions

‖M.A.P., I.M.J., and N.L.D. are equally contributing first authors. I.M.J. synthesized and characterized the NHC compounds. N.L.D. performed XPS and SEM analyses. L.C.E. performed XPS measurements. M.A.P. performed all electrochemical measurements. N.A.-C., D.M.J., and J.P.C. collaboratively designed the experiments and supervised the research. All authors contributed equally to the writing and editing of this manuscript

### Notes

The authors declare no competing financial interest.

## ■ ACKNOWLEDGMENTS

M.A.P. and N.A.-C. were supported by the National Institute of General Medical Sciences of the National Institutes of Health under Award No. R01GM140143. I.M.J. and D.M.J. were supported by the National Science Foundation under Award No. CHE 2108328. N.L.D., L.C.E., and J.P.C. were supported by the Berthiaume Institute at the University of Notre Dame and the National Science Foundation under Award No. CHE 2108330. The content is solely the

responsibility of the authors and does not necessarily represent the official views of the National Institutes of Health or the National Science Foundation. N.L.D. gratefully acknowledges the Berthiaume Institute for summer fellowship funding. The authors thank Alexander Mukasyan and Tatyana Orlova of the Notre Dame Integrated Imaging Facility for assistance with SEM imaging using the Magellan 400 SEM as well as Ian V. Lightcap and Anna Matzner of the Notre Dame Materials Characterization Facility for use of the PHI VersaProbe II XPS Instrument.

## REFERENCES

(1) Chaki, N. K.; Vijayamohanan, K. Self-Assembled Monolayers as a Tunable Platform for Biosensor Applications. *Biosens. Bioelectron.* **2002**, *17*, 1−12.
(2) Singh, M.; Kaur, N.; Comini, E. The Role of Self-Assembled Monolayers in Electronic Devices. *J. Mater. Chem. C* **2020**, *8*, 3938−3955.
(3) Wink, T.; J van Zuilen, S.; Bult, A.; P van Bennekom, W. Self-assembled Monolayers for Biosensors. *Analyst* **1997**, *122*, 43R−50R.
(4) Hahn, C. D.; Leitner, C.; Weinbrenner, T.; Schlapak, R.; Tinazli, A.; Tampé, R.; Lackner, B.; Steindl, C.; Hinterdorfer, P.; Gruber, H. J.; Hölzl, M. Self-Assembled Monolayers with Latent Aldehydes for Protein Immobilization. *Bioconjugate Chem.* **2007**, *18*, 247−253.
(5) Furst, A. L.; Hill, M. G.; Barton, J. K. DNA-Modified Electrodes Fabricated Using Copper-Free Click Chemistry for Enhanced Protein Detection. *Langmuir* **2013**, *29*, 16141−16149.
(6) Ostuni, E.; Chapman, R. G.; Liang, M. N.; Meluleni, G.; Pier, G.; Ingber, D. E.; Whitesides, G. M. Self-Assembled Monolayers That Resist the Adsorption of Proteins and the Adhesion of Bacterial and Mammalian Cells. *Langmuir* **2001**, *17*, 6336−6343.
(7) Li, H.; Dauphin-Ducharme, P.; Arroyo-Currás, N.; Tran, C. H.; Vieira, P. A.; Li, S.; Shin, C.; Somerson, J.; Kippin, T. E.; Plaxco, K. W. A Biomimetic Phosphatidylcholine-Terminated Monolayer Greatly Improves the In Vivo Performance of Electrochemical Aptamer-Based Sensors. *Angew. Chem., Int. Ed.* **2017**, *56*, 7492−7495.
(8) Li, S.; Wang, Y.; Zhang, Z.; Wang, Y.; Li, H.; Xia, F. Exploring End-Group Effect of Alkanethiol Self-Assembled Monolayers on Electrochemical Aptamer-Based Sensors in Biological Fluids. *Anal. Chem.* **2021**, *93*, 5849−5855.
(9) Green, J. D.; Clarke, E.; Porter, M. D.; McDermott, C. A.; McDermott, M. T.; Zhong, C.-J.; Bergren, A. J. On the Counter-intuitive Heterogeneous Electron Transfer Barrier Properties of Alkanethiolate Monolayers on Gold: Smooth versus Rough Surfaces. *Electroanalysis* **2022**, *34*, 1936−1952.
(10) Shaver, A.; Curtis, S. D.; Arroyo-Currás, N. Alkanethiol Monolayer End Groups Affect the Long-Term Operational Stability and Signaling of Electrochemical, Aptamer-Based Sensors in Biological Fluids. *ACS Appl. Mater. Interfaces* **2020**, *12*, 11214−11223.
(11) Malkhandi, S.; Yang, B.; Manohar, A. K.; Prakash, G. K. S.; Narayanan, S. R. Self-Assembled Monolayers of n-Alkanethiols Suppress Hydrogen Evolution and Increase the Efficiency of Rechargeable Iron Battery Electrodes. *J. Am. Chem. Soc.* **2013**, *135*, 347−353.
(12) Gooding, J. J.; Darwish, N. The Rise of Self-Assembled Monolayers for Fabricating Electrochemical Biosensors—An Interfacial Perspective. *Chem. Rec.* **2012**, *12*, 92−105.
(13) Carrascosa, L. G.; Martínez, L.; Huttel, Y.; Román, E.; Lechuga, L. M. Understanding the Role of Thiol and Disulfide Self-Assembled DNA Receptor Monolayers for Biosensing Applications. *Eur. Biophys. J.* **2010**, *39*, 1433−1444.
(14) Gooding, J. J.; Mearns, F.; Yang, W.; Liu, J. Self-Assembled Monolayers into the 21st Century: Recent Advances and Applications. *Electroanalysis* **2003**, *15*, 81−96.
(15) Pellitero, M. A.; Curtis, S. D.; Arroyo-Currás, N. Interrogation of Electrochemical Aptamer-Based Sensors via Peak-to-Peak Separation in Cyclic Voltammetry Improves the Temporal Stability and Batch-to-Batch Variability in Biological Fluids. *ACS Sens.* **2021**, *6*, 1199−1207.
(16) Pellitero, M. A.; Arroyo-Currás, N. Study of Surface Modification Strategies to Create Glassy Carbon-supported, Aptamer-based Sensors for Continuous Molecular Monitoring. *Anal. Bioanal. Chem.* **2022**, *414*, 5627−5641.
(17) Clark, V.; Pellitero, M. A.; Arroyo-Currás, N. Explaining the Decay of Nucleic Acid-based Sensors Under Continuous Voltammetric Interrogation. *Anal. Chem.* **2023**, *95*, 4974−4983.
(18) Leung, K. K.; Downs, A. M.; Ortega, G.; Kurnik, M.; Plaxco, K. W. Elucidating the Mechanisms Underlying the Signal Drift of Electrochemical Aptamer-Based Sensors in Whole Blood. *ACS Sens.* **2021**, *6*, 3340−3347.
(19) Watkins, Z.; Karajic, A.; Young, T.; White, R.; Heikenfeld, J. Week-Long Operation of Electrochemical Aptamer Sensors: New Insights into Self-Assembled Monolayer Degradation Mechanisms and Solutions for Stability in Serum at Body Temperature. *ACS Sens.* **2023**, *8*, 1119−1131.
(20) Crudden, C. M.; Horton, J. H.; Ebralidze, I. I.; Zenkina, O. V.; McLean, A. B.; Drevniok, B.; She, Z.; Kraatz, H.-B.; Mosey, N. J.; Seki, T.; et al. Ultra Stable Self-Assembled Monolayers of N-Heterocyclic Carbenes on Gold. *Nat. Chem.* **2014**, *6*, 409−414.
(21) Kaur, G.; Thimes, R. L.; Camden, J. P.; Jenkins, D. M. Fundamentals and Applications of N-heterocyclic Carbene Functionalized Gold Surfaces and Nanoparticles. *Chem. Commun.* **2022**, *58*, 13188−13197.
(22) Crudden, C. M.; Horton, J. H.; Narouz, M. R.; Li, Z.; Smith, C. A.; Munro, K.; Baddeley, C. J.; Larrea, C. R.; Drevniok, B.; Thanabalasingam, B.; et al. Simple Direct Formation of Self-Assembled N-heterocyclic Carbene Monolayers on Gold and their Application in Biosensing. *Nat. Commun.* **2016**, *7*, No. 12654.
(23) Li, Z.; Narouz, M. R.; Munro, K.; Hao, B.; Crudden, C. M.; Horton, J. H.; Hao, H. Carboxymethylated Dextran-Modified N-Heterocyclic Carbene Self-Assembled Monolayers on Gold for Use in Surface Plasmon Resonance Biosensing. *ACS Appl. Mater. Interfaces* **2017**, *9*, 39223−39234.
(24) Mayall, R. M.; Smith, C. A.; Hyla, A. S.; Lee, D. S.; Crudden, C. M.; Birss, V. I. Ultrasensitive and Label-Free Detection of the Measles Virus Using an N-Heterocyclic Carbene-Based Electrochemical Biosensor. *ACS Sens.* **2020**, *5*, 2747−2752.
(25) Singh, I.; Lee, D. S.; Huang, S.; Bhattacharjee, H.; Xu, W.; McLeod, J. F.; Crudden, C. M.; She, Z. N-Heterocyclic Carbenes Meet Toll-Like Receptors. *Chem. Commun.* **2021**, *57*, 8421−8424.
(26) Ferry, A.; Schaepe, K.; Tegeder, P.; Richter, C.; Chepiga, K. M.; Ravoo, B. J.; Glorius, F. Negatively Charged N-Heterocyclic Carbene-Stabilized Pd and Au Nanoparticles and Efficient Catalysis in Water. *ACS Catal.* **2015**, *5*, 5414−5420.
(27) Ernst, J. B.; Schwermann, C.; Yokota, G.-i.; Tada, M.; Muratsugu, S.; Doltsinis, N. L.; Glorius, F. Molecular Adsorbates Switch on Heterogeneous Catalysis: Induction of Reactivity by N-Heterocyclic Carbenes. *J. Am. Chem. Soc.* **2017**, *139*, 9144−9147.
(28) Narouz, M. R.; Osten, K. M.; Unsworth, P. J.; Man, R. W. Y.; Salorinne, K.; Takano, S.; Tomihara, R.; Kaappa, S.; Malola, S.; Dinh, C.-T.; et al. N-Heterocyclic Carbene-Functionalized Magic-Number Gold Nanoclusters. *Nat. Chem.* **2019**, *11*, 419−425.
(29) Koy, M.; Bellotti, P.; Das, M.; Glorius, F. N-Heterocyclic Carbenes as Tunable Ligands for Catalytic Metal Surfaces. *Nat. Catal.* **2021**, *4*, 352−363.
(30) Lewis, R. J.; Koy, M.; Macino, M.; Das, M.; Carter, J. H.; Morgan, D. J.; Davies, T. E.; Ernst, J. B.; Freakley, S. J.; Glorius, F.; Hutchings, G. J. N-Heterocyclic Carbene Modified Palladium Catalysts for the Direct Synthesis of Hydrogen Peroxide. *J. Am. Chem. Soc.* **2022**, *144*, 15431−15436.
(31) Stephens, L.; Padmos, J. D.; Narouz, M. R.; Al-Rashed, A.; Li, C.-H.; Payne, N.; Zamora, M.; Crudden, C. M.; Mauzeroll, J.; Horton, J. H. The Structural and Electrochemical Effects of N-Heterocyclic Carbene Monolayers on Magnesium. *J. Electrochem. Soc.* **2018**, *165*, No. G139.


https://doi.org/10.1021/acsami.3c06148
*ACS Appl. Mater. Interfaces* 2023, 15, 35701−35709

(32) Bakker, A.; Freitag, M.; Kolodzeiski, E.; Bellotti, P.; Timmer, A.; Ren, J.; Schulze Lammers, B.; Moock, D.; Roesky, H. W.; Mönig, H.; et al. An Electron-Rich Cyclic (Alkyl)(Amino)Carbene on Au(111), Ag(111), and Cu(111) Surfaces. *Angew. Chem., Int. Ed.* **2020**, *59*, 13643−13646.
(33) Navarro, J. J.; Das, M.; Tosoni, S.; Landwehr, F.; Koy, M.; Heyde, M.; Pacchioni, G.; Glorius, F.; Roldan Cuenya, B. Growth of N-Heterocyclic Carbene Assemblies on Cu(100) and Cu(111): From Single Molecules to Magic-Number Islands. *Angew. Chem., Int. Ed.* **2022**, *61*, No. e202202127.
(34) Angove, E.; Grillo, F.; Früchtl, H. A.; Veinot, A. J.; Singh, I.; Horton, J. H.; Crudden, C. M.; Baddeley, C. J. Highly Ordered N-Heterocyclic Carbene Monolayers on Cu(111). *J. Phys. Chem. Lett.* **2022**, *13*, 2051−2056.
(35) Berg, I.; Amit, E.; Hale, L.; Toste, F. D.; Gross, E. N-Heterocyclic Carbene Based Nanolayer for Copper Film Oxidation Mitigation. *Angew. Chem.* **2022**, *134*, No. e202201093.
(36) Navarro, J. J.; Das, M.; Tosoni, S.; Landwehr, F.; Bruce, J. P.; Heyde, M.; Pacchioni, G.; Glorius, F.; Roldan Cuenya, B. Covalent Adsorption of N-Heterocyclic Carbenes on a Copper Oxide Surface. *J. Am. Chem. Soc.* **2022**, *144*, 16267−16271.
(37) Franz, M.; Chandola, S.; Koy, M.; Zielinski, R.; Aldahhak, H.; Das, M.; Freitag, M.; Gerstmann, U.; Liebig, D.; Hoffmann, A. K.; et al. Controlled Growth of Ordered Monolayers of N-Heterocyclic Carbenes on Silicon. *Nat. Chem.* **2021**, *13*, 828−835.
(38) Sherman, L. M.; Finley, M. D.; Borsari, R. K.; Schuster-Little, N.; Strausser, S. L.; Whelan, R. J.; Jenkins, D. M.; Camden, J. P. N-Heterocyclic Carbene Ligand Stability on Gold Nanoparticles in Biological Media. *ACS Omega* **2022**, *7*, 1444−1451.
(39) Li, Z.; Munro, K.; Narouz, M. R.; Lau, A.; Hao, H.; Crudden, C. M.; Horton, J. H. Self-Assembled N-Heterocyclic Carbene-Based Carboxymethylated Dextran Monolayers on Gold as a Tunable Platform for Designing Affinity-Capture Biosensor Surfaces. *ACS Appl. Mater. Interfaces* **2018**, *10*, 17560−17570.
(40) Zhukhovitskiy, A. V.; Mavros, M. G.; Van Voorhis, T.; Johnson, J. A. Addressable Carbene Anchors for Gold Surfaces. *J. Am. Chem. Soc.* **2013**, *135*, 7418−7421.
(41) Amit, E.; Dery, L.; Dery, S.; Kim, S.; Roy, A.; Hu, Q.; Gutkin, V.; Eisenberg, H.; Stein, T.; Mandler, D.; et al. Electrochemical Deposition of N-Heterocyclic Carbene Monolayers on Metal Surfaces. *Nat. Commun.* **2020**, *11*, No. 5714.
(42) Choi, Y.; Park, C. S.; Tran, H.-V.; Li, C.-H.; Crudden, C. M.; Lee, T. R. Functionalized N-Heterocyclic Carbene Monolayers on Gold for Surface-Initiated Polymerizations. *ACS Appl. Mater. Interfaces* **2022**, *14*, 44969−44980.
(43) Zhong, C.-J.; Woods, N. T.; Dawson, G. B.; Porter, M. D. Formation of Thiol-based Monolayers on Gold: Implications from Open Circuit Potential Measurements. *Electrochem. Commun.* **1999**, *1*, 17−21.
(44) Góes, M. S.; Rahman, H.; Ryall, J.; Davis, J. J.; Bueno, P. R. A Dielectric Model of Self-Assembled Monolayer Interfaces by Capacitive Spectroscopy. *Langmuir* **2012**, *28*, 9689−9699.
(45) Pellitero, M. A.; Shaver, A.; Arroyo-Currás, N. Approaches for the Electrochemical Interrogation of DNA-Based Sensors: A Critical Review. *J. Electrochem. Soc.* **2020**, *167*, No. 037529.
(46) Bard, A. J. Inner-Sphere Heterogeneous Electrode Reactions. Electrocatalysis and Photocatalysis: The Challenge. *J. Am. Chem. Soc.* **2010**, *132*, 7559−7567.
(47) Inayeh, A.; Groome, R. R. K.; Singh, I.; Veinot, A. J.; de Lima, F. C.; Miwa, R. H.; Crudden, C. M.; McLean, A. B. Self-assembly of N-heterocyclic carbenes on Au(111). *Nat. Commun.* **2021**, *12*, No. 4034.
(48) Dominique, N. L.; Chen, R.; Santos, A. V. B.; Strausser, S. L.; Rauch, T.; Kotseos, C. Q.; Boggess, W. C.; Jensen, L.; Jenkins, D. M.; Camden, J. P. Ad Aurum: Tunable Transfer of N-Heterocyclic Carbene Complexes to Gold Surfaces. *Inorg. Chem. Front.* **2022**, *9*, 6279−6287.
(49) Rühling, A.; Schaepe, K.; Rakers, L.; Vonhören, B.; Tegeder, P.; Ravoo, B. J.; Glorius, F. Modular Bidentate Hybrid NHC-Thioether Ligands for the Stabilization of Palladium Nanoparticles in Various Solvents. *Angew. Chem., Int. Ed.* **2016**, *55*, 5856−5860.
(50) Jiang, L.; Zhang, B.; Médard, G.; Seitsonen, A. P.; Haag, F.; Allegretti, F.; Reichert, J.; Kuster, B.; Barth, J. V.; Papageorgiou, A. C. N-Heterocyclic Carbenes on Close-packed Coinage Metal Surfaces: Bis-Carbene Metal Adatom Bonding Scheme of Monolayer Films on Au, Ag and Cu. *Chem. Sci.* **2017**, *8*, 8301−8308.
(51) Bonsall, R. *Electrochemical Reductive Stability of Self-Assembled Monolayers on Transition Metal Electrodes*; University of Michigan, 2022.
(52) Aller Pellitero, M.; Kitsara, M.; Eibensteiner, F.; del Campo, F. J. Rapid Prototyping of Electrochemical Lateral Flow Devices: Stencilled Electrodes. *Analyst* **2016**, *141*, 2515−2522.
(53) Li, S.; Ferrer-Ruiz, A.; Dai, J.; Ramos-Soriano, J.; Du, X.; Zhu, M.; Zhang, W.; Wang, Y.; Herranz, M. Á.; Jing, L.; et al. A pH-Independent Electrochemical Aptamer-based Biosensor Supports Quantitative, Real-time Measurement *in vivo*. *Chem. Sci.* **2022**, *13*, 8813−8820.
(54) Aller Pellitero, M.; Kundu, N.; Sczepanski, J.; Arroyo-Currás, N. Os(II/III) Complex Supports pH-Insensitive Electrochemical DNA-based Sensing with Superior Operational Stability than the Benchmark Methylene Blue Reporter. *Analyst* **2023**, *148*, 806−813.
(55) Salorinne, K.; Man, R. W. Y.; Li, C.-H.; Taki, M.; Nambo, M.; Crudden, C. M. Water-Soluble N-Heterocyclic Carbene-Protected Gold Nanoparticles: Size-Controlled Synthesis, Stability, and Optical Properties. *Angew. Chem., Int. Ed.* **2017**, *56*, 6198−6202.
(56) Huynh, H. V.; Lam, T. T.; Luong, H. T. T. Anion Influences on Reactivity and NMR Spectroscopic Features of NHC Precursors. *RSC Adv.* **2018**, *8*, 34960−34966.
(57) Böhme, M. D.; Eder, T.; Röthel, M. B.; Dutschke, P. D.; Wilm, L. F. B.; Hahn, F. E.; Dielmann, F. Synthesis of N-Heterocyclic Carbenes and Their Complexes by Chloronium Ion Abstraction from 2-Chloroazolium Salts Using Electron-Rich Phosphines. *Angew. Chem., Int. Ed.* **2022**, *61*, No. e202202190.
(58) Curtis, S. D.; Ploense, K. L.; Kurnik, M.; Ortega, G.; Parolo, C.; Kippin, T. E.; Plaxco, K. W.; Arroyo-Currás, N. Open Source Software for the Real-Time Control, Processing, and Visualization of High-Volume Electrochemical Data. *Anal. Chem.* **2019**, *91*, 12321−12328.
(59) Moulder, J. F.; Stickle, W. F.; Sobol, W. M.; Bomben, K. D. *Handbook of X-Ray Photoelectron Spectroscopy*; Perkin-Elmer Corporation, 1992.
(60) Korin, E.; Froumin, N.; Cohen, S. Surface Analysis of Nanocomplexes by X-ray Photoelectron Spectroscopy (XPS). *ACS Biomater. Sci. Eng.* **2017**, *3*, 882−889.
(61) Shard, A. G. Practical guides for x-ray photoelectron spectroscopy: Quantitative XPS. *J. Vac. Sci. Technol., A* **2020**, *38*, No. 041201.
(62) Major, G. H.; Fairley, N.; Sherwood, P. M. A.; Linford, M. R.; Terry, J.; Fernandez, V.; Artyushkova, K. Practical Guide for Curve Fitting in X-Ray Photoelectron Spectroscopy. *J. Vac. Sci. Technol., A* **2020**, *38*, No. 061203.
(63) Tougaard, S. Practical Algorithm for Background Subtraction. *Surf. Sci.* **1989**, *216*, 343−360.
(64) Bearden, J. A. X-Ray Wavelengths. *Rev. Mod. Phys.* **1967**, *39*, 78−124.


https://doi.org/10.1021/acsami.3c06148
*ACS Appl. Mater. Interfaces* 2023, 15, 35701−35709